ELSEVIER

5-axis Control Ultra-precision Machining of Complex-shaped Mirrors for Extreme Ultraviolet Lithography System

H. Takino[1], T. Kawai[2], Y. Takeuchi[3] (1)
[1]Core Technology Center, Nikon Corp., Sagamihara, Kanagawa, Japan
[2]Robomachine Laboratory, FANUC Ltd., Oshino, Yamanashi, Japan
[3]Dept. of Mechanical Engineering, Graduate School of Engineering, Osaka University, Suita, Osaka, Japan

Abstract
The study deals with the manufacture of novel mirrors, an arc-shaped fly-eye mirror and a rectangular fly-eye one, for an extreme ultraviolet lithography system. Both mirrors have a complex reflective surface consisting of many small spherical mirror elements. A method is proposed to accurately realize such mirrors, using ultra-precision 5-axis control machining. The method enables to manufacture spherical surfaces with any radius, without changing the tool shape. Furthermore, another advantage of the method is that the sphericity of the resulting surfaces is independent of tool shape accuracy. By using this method, two kinds of fly-eye mirror with sixteen mirror elements are successfully fabricated.

Keywords:
Ultra-precision, Milling, Fly-eye mirror

1 INTRODUCTION

In recent years, to further minimize the line width of integrated circuit devices, an extreme ultraviolet lithography (EUVL) system is being developed, which uses a light with a short wavelength as much as 13.5 nm [1-3]. In the last few years, a new optical system for an EUVL system was designed, in which novel mirrors with complex-shaped reflective surfaces, an arc-shaped fly-eye (AF) mirror and a rectangular fly-eye (RF) mirror, are employed as key optics [4]. The fly-eye mirrors have a complex reflective surface consisting of many small spherical mirror elements. The reflective surface requires high shape accuracy and smoothness. Such complexity and requirements make the mirrors difficult to fabricate.

5-axis ultra-precision milling has been attracting considerable interest because of its machining capability of three-dimensional small parts with complex shapes [5-8]. Therefore, such milling techniques have already been applied to the fabrication of the fly-eye mirrors [9]. This paper describes 5-axis control ultra-precision milling with a newly developed diamond tool. The effectiveness and practicability of the method is demonstrated in manufacturing fly-eye mirrors; AF and RF mirrors with sixteen mirror elements. The fabricated mirrors are tested to evaluate their optical characteristics using an optical testing system with visible rays.

2 FLY-EYE MIRRORS

Figure 1 shows two types of fly-eye mirror. The mirrors have a complex reflective surface consisting of approximately 500 concave mirror elements that are arranged side by side. For the AF mirror, the reflective surface of each mirror element is a part of a concave sphere, and the top of the element is arc-shaped. Although all of the mirror elements have the same arc-shaped contour, the shift value of Δx_a, which is the amount of shift from the bottom of the sphere, is not the same for all mirror elements. For the RF mirror, the reflective surface of each mirror element is also a part of a concave sphere, but the top of the element is rectangular. The shift value of Δx_r is not the same for all mirror elements, similarly to the AF mirror.

The function of the fly-eye mirrors in the proposed EUVL system is as follows: Two types of fly-eye mirror are placed, facing each other, as shown in Figure 2. In this arrangement, when the collimated ray from a light source is projected onto the AF mirror, each mirror element reflects the ray towards the RF mirror. The ray reflected on one arc-shaped mirror element is projected onto the corresponding rectangular mirror element. Then, each ray reflected by the rectangular mirror element illuminates a certain arc field on a mask through a condenser optic. In this manner, the arc field can be illuminated uniformly owing to the integration of each ray even if the ray from the light source to the AF mirror has an uneven intensity distribution.

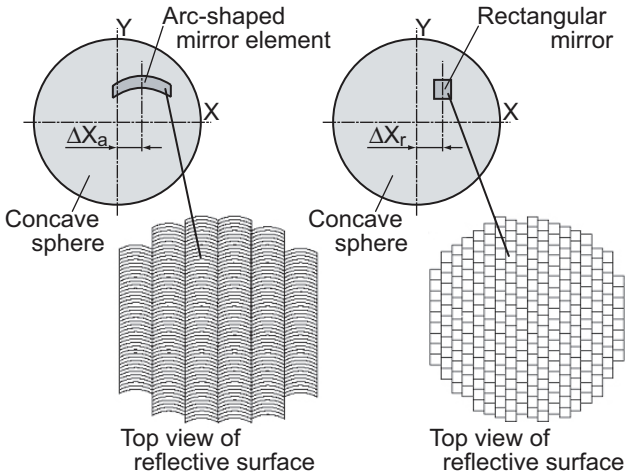

(a) Arc-shaped fly-eye mirror (b) Rectangular fly-eye mirror

Figure 1: Fly-eye mirrors.

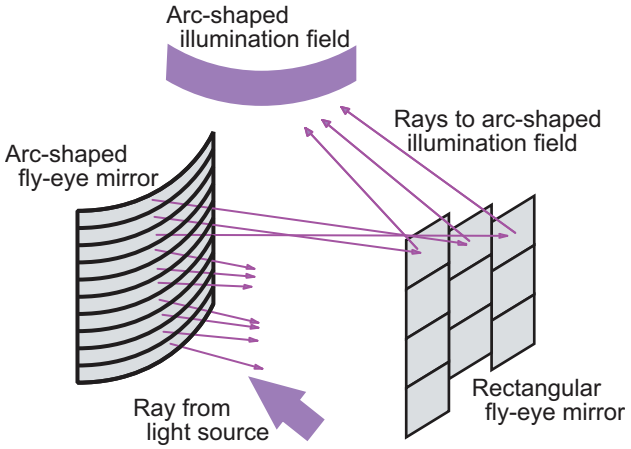

Figure 2: Illumination of an arc-shaped field using fly-eye mirrors.

 doi:10.1016/j.cirp.2007.05.031

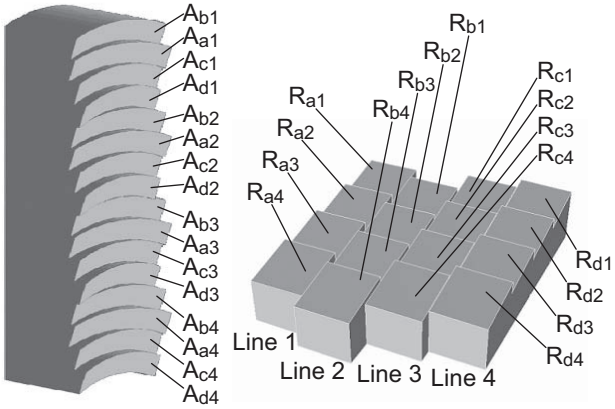

(a) Arc-shaped mirror (b) Rectangular mirror

Figure 3: Schematic of fly-eye mirrors fabricated in this study.

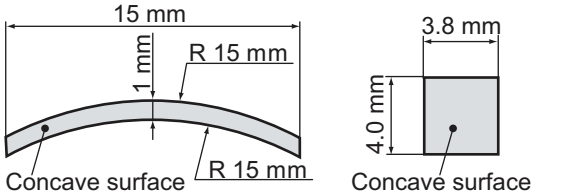

(a) Arc-shaped mirror element (b) Rectangular mirror element

Figure 4: Surface geometry of mirror elements fabricated in this study.

In the present study, the AF and RF mirrors schematically shown in Figure 3, are fabricated. Each mirror was constructed from four types of mirror element and the total number of mirror elements is sixteen. Here, the AF mirror element is represented as A_{ij} (i=a, b, c, d; j=1, 2, 3, 4), where i represents the type of mirror element. When the mirror elements have the same value of i, their shift values Δx_a are the same, where j represents the number of the mirror element, and is assigned to each type of mirror element in turn. The RF mirror shown in Figure 3(b) optically corresponds to the AF mirror shown in Figure 3(a), whose mirror elements are represented as R_{ij} (i=a, b, c, d; j=1, 2, 3, 4). The dimensions of the top of the mirror elements are shown in Figure 4.

3 FABRICATION METHOD

The AF and RF mirrors are manufactured so that the surfaces of the mirror elements are shaped in line on a block using an ultra-precision 5-axis milling machine with a diamond cutting tool, and then the blocks are connected to each other side by side to assemble the fly-eye mirror. The concept of a shaping method of their mirror surfaces has already reported, and its potential was shown through preliminary experiments [9]. In the present study, the AF and the RF mirrors with sixteen mirror elements are fabricated to confirm the feasibility of our plan on production. In the following subsections, the shaping method of the mirror surfaces is described.

3.1 Shaping principle of mirror surfaces

Figure 5 shows a tool proposed for shaping the fly-eye mirror surfaces. The tool has a cutting blade made of single-crystal diamond, whose edge is 90° or less in angle. This tool is used as an end mill by rotating it around its axis. Since the blade edge inscribes a circle by rotation, the material removal is performed at the circle. In geometry, a circle can make contact with a spherical surface with any radius. Thus, this tool enables the shaping of any radius by

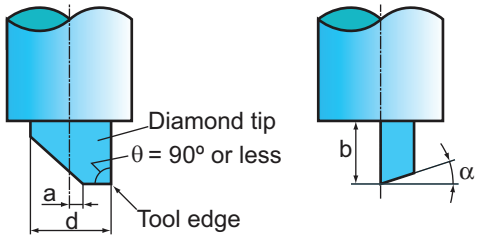

(a) Front view (b) Side view

Figure 5: Configuration of a newly designed single-crystal diamond tool.

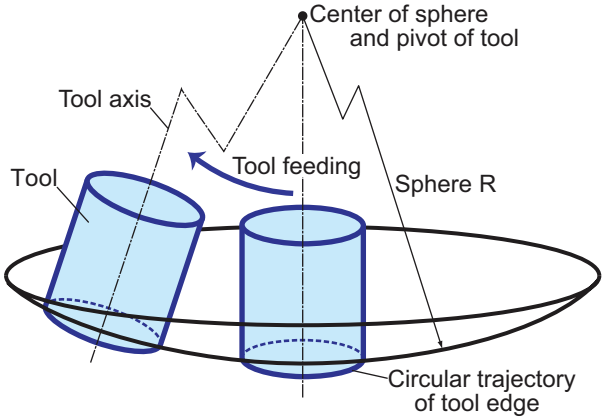

Figure 6: Shaping of a spherical surface by the new tool.

feeding the tool in such a way that the circular trajectory of the tool edge moves along the desired spherical surface, as shown in Figure 6. To shape a desired radius, the pivot of the tool is fixed at the center of the desired spherical surface during tool feeding, and the distance between the tool edge and the center of the sphere is set to be equal to the desired radius.

Although a ball-end mill is usually applied to the mirror shaping, it is not practical to shape the fly-eye mirrors by transferring the radius shape of a ball-end mill onto the mirror surface. This is because it is difficult to manufacture a ball-end mill having a desired radius with high shape accuracy, specially or particularly large radii such as a fly-eye mirror surface. On the other hand, for the proposed tool, since the removal is performed by only the tool edge, the shape accuracy of the machined surface is not affected by the tool shape, which is another advantage of the proposed tool.

3.2 Fabrication of fly-eye mirrors

Figure 7 shows the schematic of a shaping method of the fly-eye mirrors. For the shaping of AF mirror, as shown in Figure 7(a), the tool is fed along the arc of the outline of the mirror element under 5-axis motion control. For the RF mirror, the tool is moved across a block so as to shape rectangular contours with spherical surfaces, as shown in Figure 7(b). In this process of the RF mirror, although the contour is rectangular, the tool should be also fed under 5-axis motion control in such a way that the trailed circle of the tool edge runs over a spherical surface. In addition, the tool dimension is set so that the diameter of the circular trajectory of the edge can be equal to the width of the mirror element. This allows us the shaping of an entire surface of the mirror element by one feeding of the tool.

In the present work, at first the mirror elements were roughly shaped successively from end to end on the basis of the principle above mentioned. In the rough cutting process, repetitive tool feed increment was necessary for each mirror element because the depth of cut per one feed increment was set to be 50 μm. After rough cutting, finish cutting was

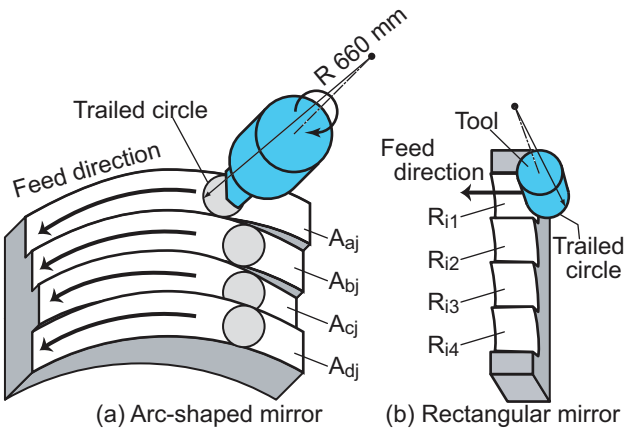

(a) Arc-shaped mirror (b) Rectangular mirror

Figure 7: Tool feeding method for reflective surfaces.

performed to improve the surface smoothness in the same manner of the rough cutting. The depth of cut of the finish cut was 0.6 μm.

The tool for the shaping of AF mirrors had a configuration of θ=90º, d=1 mm, a=20 μm, b=1 mm, α=5º and an edge radius of 30 μm in Figure 5. The tool for the RF mirrors had a configuration of θ=80º. The workpieces were brass blocks plated with copper of 1 mm in thickness, and the plated copper was shaped into the mirror surfaces under the finish cutting condition of feed rate 1 mm/min, depth of cut 0.6 μm and spindle rotation 45000 min^{-1}. We used a 5-axis ultra-precision cutting machine (Robonano, Fanuc Ltd.) having translational axis resolution of 1 nm and rotational axis resolution of 0.00001º [5-8]. For the RF mirror, four mirror elements were shaped on one block as described above. Then, the four blocks were assembled side by side on a flat plate to construct the RF mirror.

4 FABRICATION RESULTS

4.1 Arc-shaped fly-eye mirror

Figure 8 shows a photograph of the fabricated arc-shaped fly-eye mirror and a SEM image of its edges and corners. The SEM image reveals that the edges were formed sharp. The corners were round, which were due to the tool edge with a radius. Such round regions of the corners are within the permissible range of errors for the specifications of the mirror element.

The sphericity of the mirror surfaces (that is, the deviation of the machined surface from its best fit sphere) was measured, using a Fizeau-type interferometer. Figure 9 shows an example of the measured results, which revealed the peak-to-valley (PV) and rms shape accuracies to be 0.12 μm and 0.020 μm, respectively. The measured result demonstrates that the present method enables the shaping of the spherical surfaces with arc-shaped contours. Moreover, the surface topographies of the mirror surfaces within an area of 1.42 mm × 1.06 mm were measured, using an optical surface profiler. It showed that the radius of the machined surface was 627 mm, which is almost identical to the desired radius value. As a result, the proposed method can shape the arc-shaped mirror surface with high accuracy.

Then, surface roughness profiles with in an area of 1.42 mm × 1.06 mm were measured. Examples of the measured results were shown in Figure 10. Figure 10(a) shows the profiles of the mirror element A_{a2} and A_{a4}. Figure 10(b) shows the profiles of the mirror element A_{c1} and A_{c3}. These profiles are at the position of 2 mm from the edge of the mirror elements, as shown in the inset. The measurements prove that the machined surfaces have waviness with the amplitude of 30 to 50 nm. Moreover, the same type of the

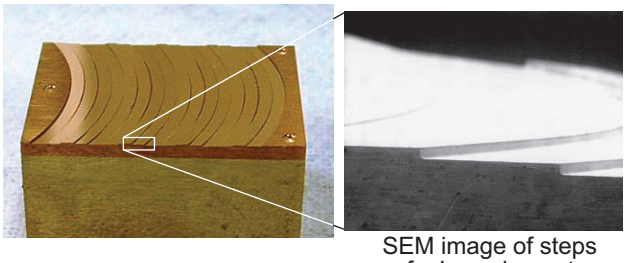

Figure 8: Photographs of a fabricated arc-shaped fly-eye mirror.

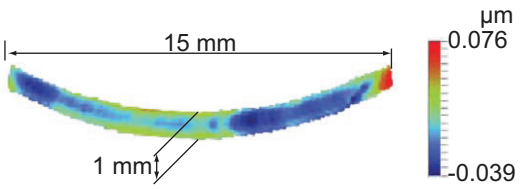

Figure 9: Sphericity of a reflective surface of an arc-shaped mirror element measured with an interferometer.

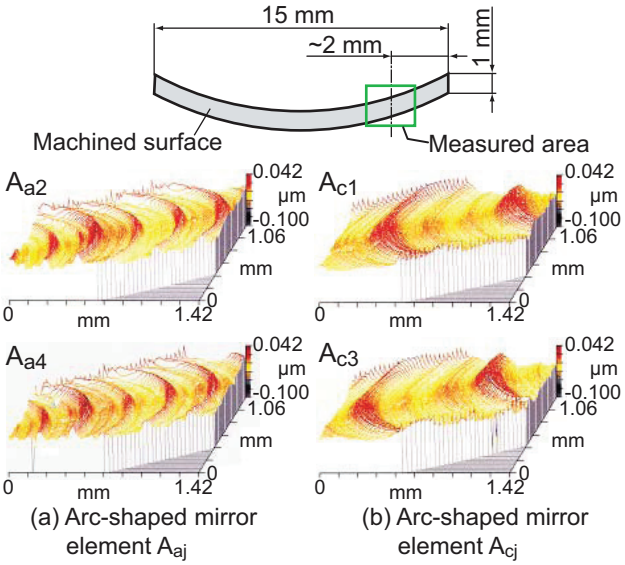

(a) Arc-shaped mirror element A_{aj} (b) Arc-shaped mirror element A_{cj}

Figure 10: Wavinesses on the machined surfaces of the arc-shaped mirror elements.

mirror element has the similar waviness profile. Such waviness possibly results from the feeding mechanism of the machine tool used.

4.2 Rectangular fly-eye mirror

Figure 11 shows a photograph of the fabricated RF mirror, and a SEM image of its edges and corners. The rounding of the corners was formed by the tool edge, as is the same as that of the AF mirror's corners, and are also out of the optical effective area of the RF mirror.

Figure 12 shows the sphericity of the mirror surface measured by the interferometer, which reveals the PV and rms shape accuracies to be 0.16 μm and 0.030 μm, respectively. Moreover, measured results by use of an optical surface profiler show that the radius of the machined surfaces was 667 mm, thus proving that the desired radius was almost achieved. As a result, it was clear that the RF mirror elements were also machined with high accuracy by the present method.

The measured surface roughness within an area of 1.42 mm × 1.06 mm shows that the waviness profiles are similar each other for the same type of the mirror, as is the same

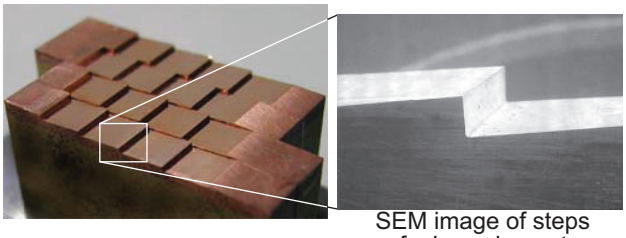

Figure 11: Photographs of a fabricated rectangular fly-eye mirror.

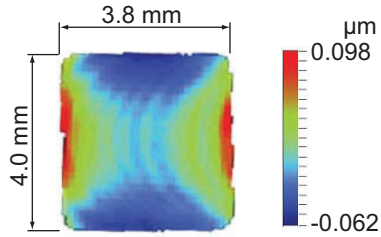

Figure 12: Sphericity of a reflective surface of a rectangular mirror element measured with an interferometer.

as that for the AF mirror elements. The amplitude of the waviness ranges from 20 to 90 nm.

5 EVALUATION OF OPTICAL CHARACTERISTICS OF FABRICATED FLY-EYE MIRRORS

5.1 Testing system

The optical characteristics of the fabricated AF and RF mirrors were evaluated, using a testing system developed in the study. The fabricated mirrors were subjected to test in order to examine the integration of illumination lights from every pair of AF and RF mirror element.

In the testing system, visible rays from a halogen lamp are introduced into collimator optics through an optical fiber. The parallel rays from the collimator optics are reflected by the AF mirror and the RF mirror. The rays reflected from every RF mirror element are introduced into the condenser optics, and then are projected on a CCD camera and are processed by a computer. If the AF and RF mirrors are fabricated with high accuracy, the rays are projected at the same position on CCD camera, thus leading to the integration of the rays. This examination models the integration of rays on a mask in a EUVL system.

5.2 Evaluation results

Figure 13 shows the left part of the illumination light observed by the CCD camera. It is found that illumination lights from every mirrors element are almost integrated on the same area, thus proving that the mirrors fabricated in the present study achieved the important optical function of the fly-eye mirror. However, the integrated light has a nonuniform intensity distribution, as shown in the same figure. The calculation on the basis of the optical magnitude of the testing system shows that the intensity pattern on the illumination is related to the waviness on the arc-shaped mirror element. The waviness on the arc-shaped mirror element should be reduced since the illumination intensity is required to be as uniform as possible.

6 CONCLUSIONS

The study is summarized as follows:

1. The proposed shaping method including a newly designed diamond tool and its 5-axis feeding method is capable of forming spherical surfaces with an arc-shaped or a rectangular contour.

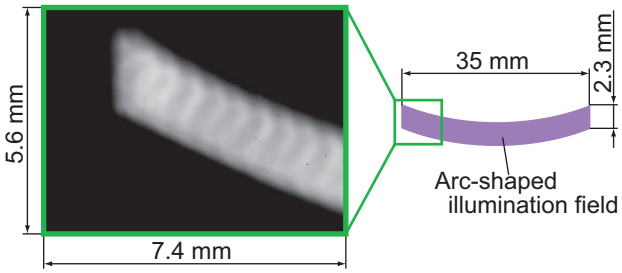

Figure 13: Illumination intensity distribution produced by 16 pairs of mirror elements.

2. Arc-shaped and rectangular fly-eye mirrors with sixteen mirror elements are successfully fabricated by the proposed method, demonstrating the practicability of the proposed method for actual mirror production.
3. The important optical function of the fly-eye mirrors, that is, the integration of the rays from a light source, was realized by the fabricated fly-eye mirrors.
4. The surfaces of the fabricated mirror elements have waviness with a height on the order of ten nanometers, causing uneven illumination intensity. Thus, the waviness must be removed to achieve superior optical performance.

7 ACKNOWLEDGEMENTS

The authors would like to thank Mr. Y. Hashimoto and Mr. T. Sumita of University of Electro-Communications for performing machining experiments. They also acknowledge Mr. K. Nomura of Nikon Corp. for useful discussions.

8 REFERENCES

[1] Sweatt, W. C., 1993, High-efficiency Condenser Design for Illuminating a Ring Field, OSA Proc. on Soft X-ray Projection Lithography, 18/70-72.

[2] Murphy, J. B., White, D. L., McDowell, A. A., Wood II, O. R., 1993, Synchrotron Radiation Sources and Condensers for Projection X-ray Lithography, Appl. Opt. 32/6920-6929.

[3] Chapman, H. N., Nugent, K. A., 1999, A Novel Condenser for EUV Lithography Ring-Field Projection Optics, Proc. SPIE, 3767/225-236.

[4] Komatsuda, H., 2000, Novel illumination system for EUVL, Proc. SPIE, 3997/765-776.

[5] Takeuchi, Y., Miyagawa, O., Kawai, T., Sawada, K., Sata, T., 2001, Non-adhesive Direct Bonding of Tiny Parts by Means of Ultraprecision Trapezoid Microgrooves, Journal of Micro system Technologies, Springer-Verlag, 7/1: 6-10.

[6] Takeuchi, Y., Maeda, S., Kawai, T., Sawada, K., 2002, Manufacture of Multiple-focus Micro Fresnel Lenses by Means of Non rotational Diamond Grooving, Annals of the CIRP, 51/1: 343-346.

[7] Takeuchi, Y., Yonekura, H., T., Sawada, K., 2003, Creation of 3-D Tiny Statue by 5-Axis Control Ultraprecision Machining, Computer-Aided Design, Elsevier, 35/4: 403-409.

[8] Takeuchi, Y., Suzukawa, H. Kawai, T., Sakaida, Y., 2006, Creation of Ultra-precision Microstructures with High Aspect Ratios, Annals of the CIRP, 55/1: 107-110.

[9] Hashimoto, Y., Takeuchi, Y., Kawai, T., Sawada, K., Takino, H., Nomura, K., 2004, Ultraprecision 5-axis Control Machining of Fly-eye Mirror in EUV Lithography, JSME International Journal, 47/3: 916-924.